Ghostbursting in sensory cells of electric fish

Carlo R. Laing
Institute of Information and Mathematical Sciences, Massey University,
Private Bag 102-904, North Shore Mail Centre, Auckland, New Zealand
November 4, 2003

AMS Subject classification: 92C20, 37N25, 34C15
Key words: Bursting, electric fish, sensory processing, integrate–and–fire.

Abstract: We give an overview of the analysis of a new type of bursting ("ghostbursting") seen in pyramidal cells of weakly electric fish. We start with the experimental observations and characterization of the bursting, describe a compartmental model of a pyramidal cell that undergoes ghostbursting and the development of a simplified yet realistic conductance–based model of this cell. This model then motivates a minimal leaky integrate–and–fire model that also has the qualitative features of ghostbursting.

1 Introduction

Bursting, the slow alternation between spiking behavior and quiescence, is a common cellular phenomenon [7, 8]. It was recognised early on that not all bursting is qualitatively the same, and early classifications of bursting systems reflected their qualitative nature, e.g. parabolic or square–wave bursting [16]. An almost universal assumption in the mathematical analysis of bursting systems was that the system could be decomposed into two subsystems, a "fast" subsystem and a "slow" subsystem, and that when the variables in the slow subsystem were held constant the fast subsystem either oscillated or was quiescent [7, 16]. The slow variables were assumed to be driven by the dynamics of the fast subsystem and thus bursting could be viewed as a slow cycling through phase space, with the fast subsystem periodically moving from a spiking regime to a quiescent one and back again.

While this approach has been very successful, a new type of bursting — referred to as "ghostbursting" — which does not fit into any of the previous categories for bursting types has been recently investigated [4]. Ghostbursting occurs under constant current injection in *in vitro* preparations of pyramidal cells from the electrosensory lateral line lobe (ELL) of the weakly electric fish *Apteronotus leptorhychus*. These cells receive direct synaptic input from electroreceptors on the fish's skin which detect the amplitude modulation of a self–generated electric field around the fish [2], and are thus near the start of the electrosensory processing system. Here we give a brief summary of the stages in the study of this type of bursting.

What is now referred to as ghostbursting was observed in the early 1990s [18]. An example of a typical experimental recording is shown in Figure 1. Several features are apparent. The most prominent is the monotonic decrease in interspike intervals (ISIs) during the burst. This is in contrast with most other types of bursting in which there is either an increase of ISIs during a burst, a decrease and then an increase, or no particular trend [7, 8, 16]. Another interesting feature of the bursting shown in Figure 1 is the slow rise in the minimum voltage between spikes during a burst and the sudden drop in the voltage after the final spike in a burst.

In Ref. [18] it was determined that there were active ion channels in the dendrite of these pyramidal cells, and that the interaction between somatic and dendritic action potentials was

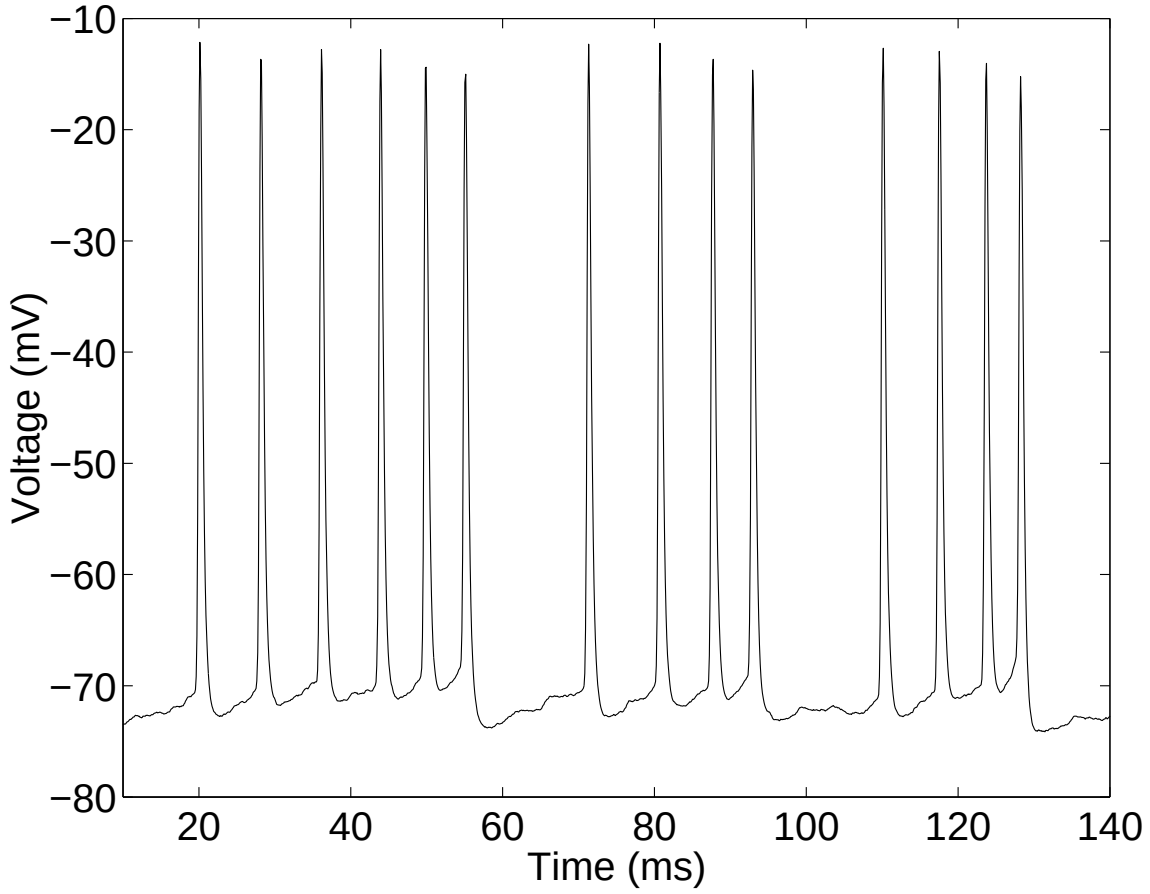

Figure 1: Somatic membrane potential as a function of time for a pyramidal cell from the ELL of *A. leptorhychus*. This is part of a 4 sec long recording, during which a constant current of 0.8 nA was injected. Three bursts are shown. Data provided by Anne-Marie Oswald.

a necessary component of the bursting. These authors observed that most somatic action potentials were followed by a depolarizing afterpotential (DAP) of similar duration to the dendritic action potential, and that during repetitive firing the DAPs could increase in amplitude, resulting in progressively shorter interspike intervals and an increase in the minimum voltage between spikes in a burst [13]. This process of DAP growth was terminated when a very short ISI (a "doublet") occurred at the soma, which was followed by a long ISI. These long ISIs thus grouped the action potentials into bursts (see Figure 1). The existence of DAPs in Figure 1 is inferred, since without them the voltage after each action potential would drop to a lower value, similar to that seen immediately after each doublet.

Further work [13] determined that the dendritic refractory period was longer than the somatic, and the termination of a burst occurred when a somatic ISI (the doublet) was shorter in duration than the dendritic refractory period and the dendrite could not produce an action potential in response to the second of the two somatic action potentials forming the doublet. It was also determined that the pyramidal cells switched from periodic to burst firing as the injected current was increased (in contrast with many other types of bursting [8, 15]), and that the duration of bursts (once they occurred) decreased as current increased.

2 A Large Compartmental Model

The first model of a neuron capable of ghostbursting was presented in [5]. This was a "compartmental" model, in which a particular neuron was photographed and the main features of its morphology digitized, so that a "virtual neuron" could be constructed within a computer. The neuron was necessarily represented as a finite number of isopotential compartments (over 300), and appropriate ion channels were distributed over the compartments. The exact nature of these channels was chosen so as to match experimental recordings of individual action potentials as closely as possible, with some parameters being estimated from previous experimental work. Doiron et al. [5] found that to successfully reproduce the experimentally observed burst patterning they had to include a slow cumulative inactivation of the repolarizing potassium current in the dendrite.

While this large compartmental model was very realistic, it was too complex for many such neurons to be simulated at the same time (for example, in a simulation of a network of neurons) and more importantly, it was very difficult to understand the "essence" of bursting in the model in the same way that bursting in minimal models can be understood [16]. Thus the next stage was to create a minimal model which reproduced the qualitative (and to a large extent, quantitative) behavior of the large model just discussed. This minimal model would be easier to analyse than the large compartmental model, and could be used in the implementation of a large–scale network simulation. This would be of interest, as the pyramidal cells discussed here receive different inputs depending on their position within the ELL, and also receive much feedback from other brain structures [1]. Their role in these networks has only recently been studied [3].

3 The "ghostburster"

In order to reduce the large compartmental model [5] to a minimal model several things were done. Firstly, the entire dendrite, which was represented by all but one of the compartments in the large compartmental model, was represented as a single compartment. The soma was represented by another compartment, resulting in a two–compartment model, similar to that

in [15]. Secondly, the ion channels not thought to be necessary for the bursting behavior were eliminated. Crucially, it was important *not* to eliminate the dendritic potassium current, as it is thought that the presence of this current underlies the bursting discussed here. Thirdly, previously–used simplifications were used to further reduce the number of variables. (Specifically, it was assumed that the activation of sodium channels is instantaneous. Also, use was made of the observation that $h_s + n_s$ is approximately equal to 1 during an entire action potential [4, 8], where h_s is the somatic sodium inactivation variable and n_s is the somatic potassium activation variable.)

The resulting equations, presented in [4], are

$$\begin{aligned}
C\frac{dV_s}{dt} &= I - g_{Na,s}[m_{\infty,s}(V_s)]^2(1-n_s)(V_s - V_{Na}) - g_{dr,s}n_s^2(V_s - V_K) \\
&\quad -g_L(V_s - V_L) - \frac{g_c}{\kappa}(V_s - V_d) && (1)\\
\frac{dn_s}{dt} &= \frac{n_{\infty,s}(V_s) - n_s}{0.39} && (2)\\
C\frac{dV_d}{dt} &= -g_{Na,d}[m_{\infty,d}(V_d)]^2 h_d(V_d - V_{Na}) - g_{dr,d}n_d^2 p_d(V_d - V_K) \\
&\quad -g_L(V_d - V_L) - \frac{g_c}{1-\kappa}(V_d - V_s) && (3)\\
\frac{dh_d}{dt} &= h_{\infty,d}(V_d) - h_d && (4)\\
\frac{dn_d}{dt} &= \frac{n_{\infty,d}(V_d) - n_d}{0.9} && (5)\\
\frac{dp_d}{dt} &= \frac{p_{\infty,d}(V_d) - p_d}{5} && (6)
\end{aligned}$$

Subscripts s and d refer to somatic and dendritic variables, respectively. Equations (1) and (3) are current balance equations for the soma and dendrite of the neuron, respectively, and the other equations govern the ion channel dynamics. The variables m and h are activation and inactivation of Na^+, respectively, and n and p are activation and inactivation of K^+, respectively. Parameter values are $C = 1$, $g_{Na,s} = 55$, $V_{Na} = 40$, $g_{dr,s} = 20$, $V_K = -88.5$, $g_L = 0.18$, $V_L = -70$, $g_c = 1$, $\kappa = 0.4$, $g_{Na,d} = 5$, $g_{dr,d} = 15$. I is the somatic input current, g_c is the coupling conductance, and κ is the ratio of the somatic area to the total area of the cell. Other functions are $m_{\infty,s}(V) = 1/[1 + \exp(-(V+40)/3)]$, $n_{\infty,s}(V) = 1/[1 + \exp(-(V+40)/3)]$, $m_{\infty,d}(V) = 1/[1 + \exp(-(V+40)/5)]$, $h_{\infty,d}(V) = 1/[1 + \exp((V+52)/5)]$, $n_{\infty,d}(V) = 1/[1 + \exp(-(V+40)/5)]$, $p_{\infty,d}(V) = 1/[1 + \exp((V+65)/6)]$. Note that these functions and parameter values are the same as used in the large model [5].

An example of the behaviour of (1)-(6) is shown in Figure 2 for $I = 10$. Note that the dendritic action potentials are wider than the somatic. During a burst, the dendritic potassium inactivation variable p_d slowly decreases, resulting in the progressive widening of the dendritic action potentials and the decrease in ISIs. There are several differences between the results plotted in Figure 2 and the experimental results in Figure 1 and elsewhere. For example, the minimum somatic voltage between action potentials in the experimental recordings gradually rises during a burst, whereas such a rise is not seen in the model results. Also, experimental recording show a slow decrease in the amplitude of dendritic action potentials during a burst [4, 5], whereas this does not appear in Figure 2. These are minor discrepancies that do not affect the understanding of the mechanisms involved in the bursting, and overall, the model (1)-(6) qualitatively, and to a large extent quantitatively, reproduces the bursting seen both in experiments [13] and in the large compartmental model [5].

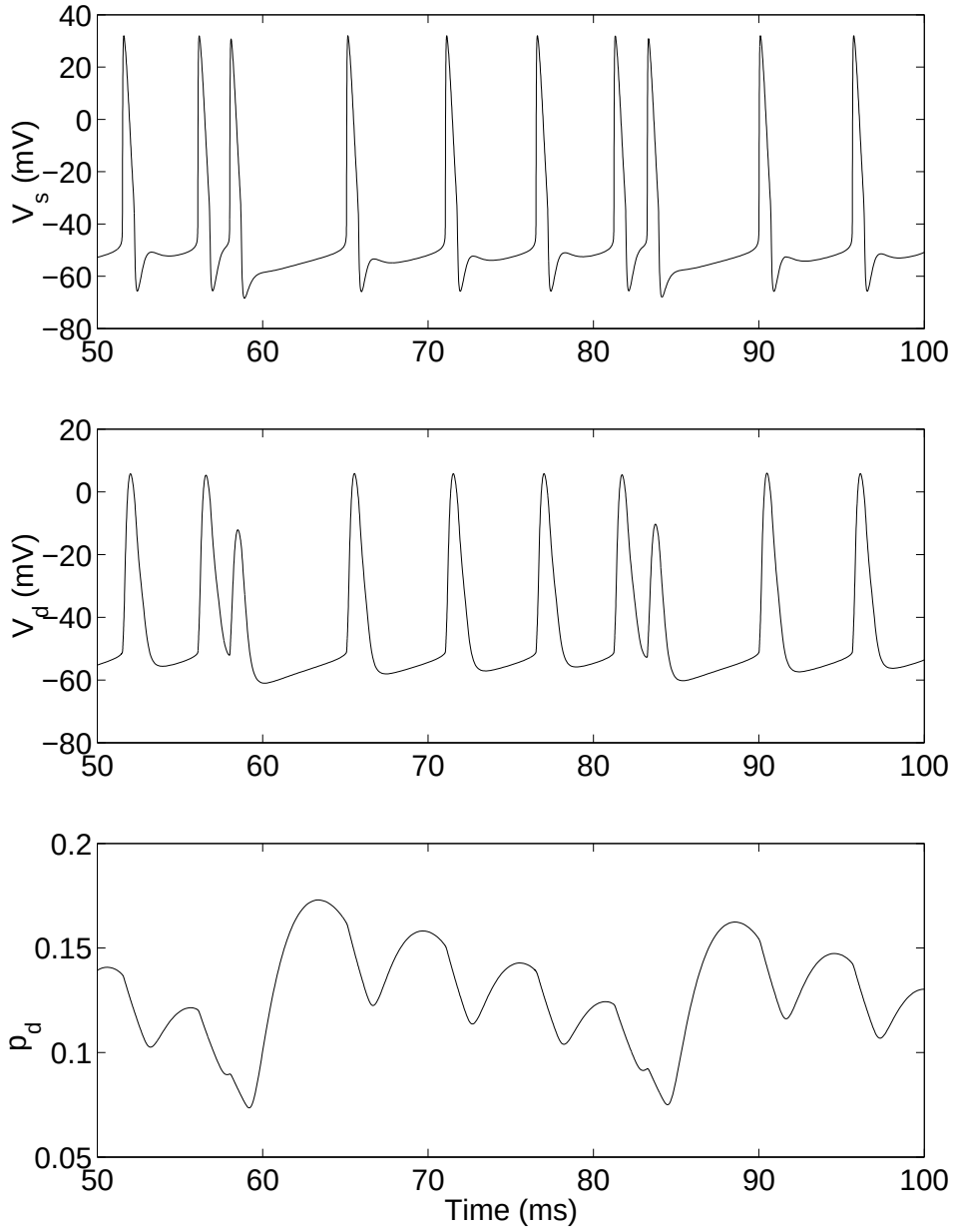

Figure 2: An example of ghostbursting in (1)-(6). Top: somatic voltage, middle: dendritic voltage, bottom: dendritic potassium inactivation. The full burst shown starts at $t \approx 60$ and ends at $t \approx 85$ with a high frequency "doublet". $I = 10$. Note the reduced dendritic voltage in the second action potential of the doublet, and the DAPs (the small rise and then fall in voltage) that occur after most somatic action potentials. The bursting is chaotic, as the maximal numerically-determined Lyapunov exponent is positive [4]; thus no two bursts are identical.

As I is increased in (1)-(6), the system moves from quiescence to periodic firing of action potentials (spikes) to bursting, in the same way as the large model [5] and real neurons [10, 13]. The small number of variables in (1)-(6) allowed the authors to determine that the bifurcation separating periodic from burst firing was a saddle–node bifurcation of periodic orbits [4]. One of the implications of this is that the length of a burst should scale as the inverse square root of the amount by which the system is above the periodic/burst threshold. This provides an explanation for the observation that burst duration decreased as current was increased [13].

In [4] the effect of varying the conductance $g_{dr,d}$ (in Eqn. (3)) was studied, and it was shown that by varying both $g_{dr,d}$ and the injected current I burst patterns with a variety of lengths and interburst intervals could be obtained. This was understood in terms of a bifurcation analysis of (1)-(6) using $g_{dr,d}$ and I as bifurcation parameters.

Despite there being no actual slow subsystem in (1)-(6) (the longest time constant is 5 ms) some insight was gained by treating p_d as a slow variable and studying the "fast" subsystem (1)-(5) with p_d as a parameter. It was found that as p_d was gradually reduced the fast subsystem abruptly switched from simple periodic behavior to a periodic oscillation in which the variables had *two* maxima per period; see Figure 3. In this "period–two" phase the second somatic action potential in the doublet falls within the dendritic refractory period and thus the dendrite cannot fully respond to it. In analogy with the usual "slow–fast" analysis of bursters [7, 16], p_d can be thought of as being driven down by the period–one behavior until the full system enters the period two regime, leading to the failure of the dendrite to respond to a somatic action potential, which then creates a long ISI in which p_d recovers to its value at the start of the next burst (see Figure 2).

Figure 3 shows the behavior of the fast subsystem (1)-(5) when p_d is held constant. The sudden change from period-one to period-two behavior as p_d decreases through ~ 0.1 is seen by plotting the local maxima of V_d during one period. The p_d nullcline (obtained from $V_d = p_{\infty,d}^{-1}(p_d)$, see eqution (6)) is also plotted, and a single burst of the full system (1)-(6) is superimposed.

The ghostburster does not fit into any previous categorizations of bursting neurons [7] since the fast subsystem is not bistable for any fixed values of the slow subsystem, yet the slow subsystem has only one variable (p_d). Also, one of the bifurcations involved in bursting (the period–one to period–two transition mentioned above) has not been previously regarded as a possible relevant component of a bursting system. Another interesting point is that the apparently slow segment of a burst (the interburst interval) is not due to a slow variable in the model but rather to the system's passage in phase space close to a saddle–node bifurcation. This is the origin of the name "ghostburster", as such a motion has been referred to as sensing the "ghost" of a saddle–node bifurcation [17].

4 A minimal model

While the model (1)-(6) qualitatively and largely quantitatively reproduced the behaviour seen in the large model of [5], it still involves six variables, resulting in difficulties when trying to visualize the system's phase space. The next step was to create a minimal model that kept only the qualitative features of ghostbursting and which had as few variables as possible. A one–variable "integrate and fire" neuron was chosen to provide the action potentials for the model, and a second variable (c) was added whose modulation would give rise to the bursting patterns [11].

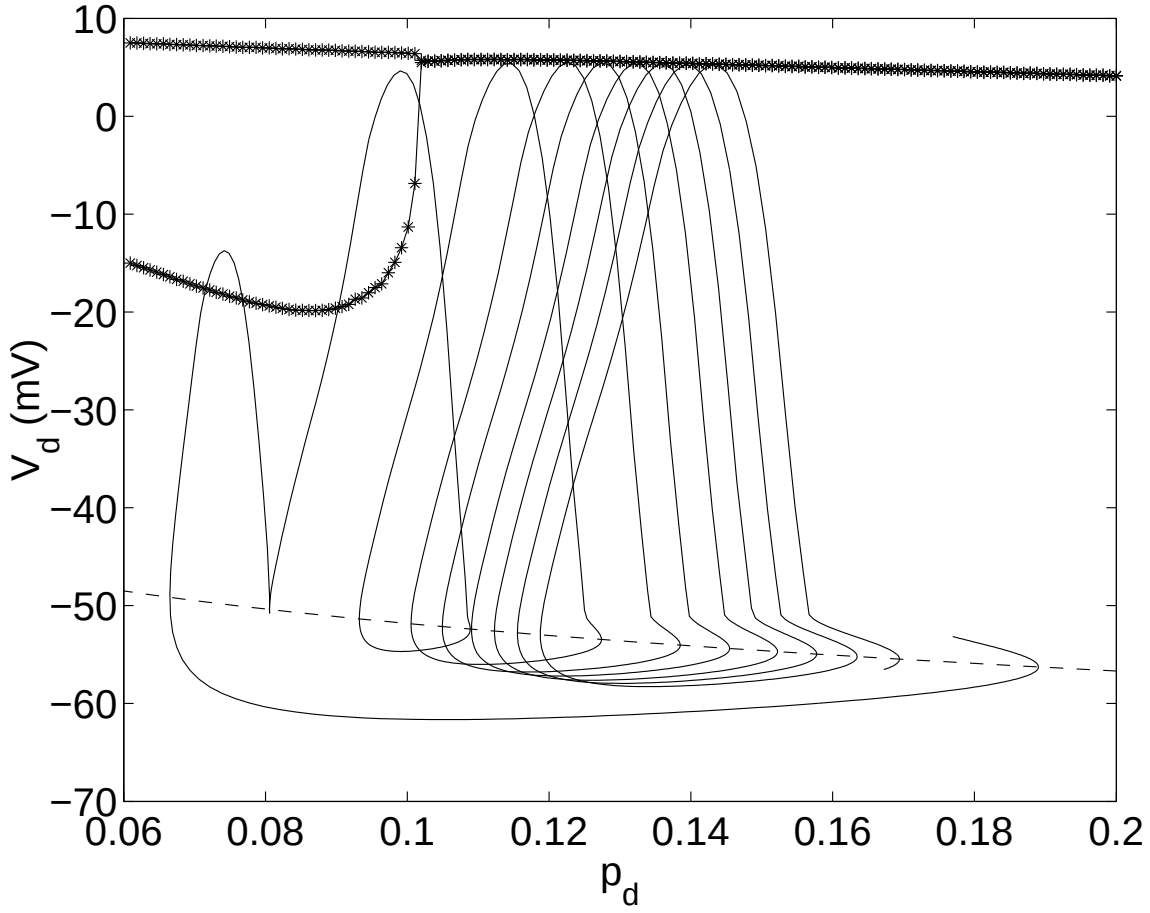

Figure 3: One burst of the system (1)-(6) superimposed over a "skeleton" obtained by using p_d as a bifurcation parameter and studying the fast system (1)-(5). Joined stars: local maxima of V_d. Dashed: nullcline for p_d; above this line $dp_d/dt < 0$, below this, $dp_d/dt > 0$. Solid line: the trajectory of one burst. See text for discussion. $I = 9$.

In the ionic models, the dendritic action potential halfwidth is greater than that of the somatic, and the effect of this is that a short time after each somatic spike (except for the second one in a doublet), a depolarizing current flows from the dendrite to the soma. This "delayed feedback" was implemented in the minimal model with an actual delay. The failure of the dendrite to respond to a somatic action potential was implemented with a simple comparison between the last ISI and the dendritic refractory period, and the effective DAP height was used to instantaneously increment the effective somatic voltage.

The equations chosen for the minimal model were

$$\frac{dV}{dt} = I - V + c\sum_n H(t_n - t_{n-1} - r)\delta(t - t_n - \sigma) \tag{7}$$

$$\frac{dc}{dt} = -c/\tau + (B + Cc^2)\sum_n \delta(t - t_n) \tag{8}$$

with the rule $V(t_n^+) = 0$ if $V(t_n^-) = 1$, and the t_n are the times at which the reset occurs (n is an integer). V represents the somatic membrane potential, I is the current injected to the soma, $H(\cdot)$ is the Heaviside function [$H(x) = 0$ if $x < 0$, and $H(x) = 1$ if $x \geq 0$], r represents the refractory period of the dendrite, σ is the effective delay between the somatic action potential and the dendritic–to–somatic current that causes the DAP, and B, C and τ are constants. $\delta(\cdot)$ is the Dirac delta function which is zero except when its argument is zero. The action potentials are thought of as occurring at the times t_n. (Note that the original presentation in [11] had another parameter multiplying the c in (7), but this can be scaled out and we have done that here.)

An example of this model's behaviour during bursting is shown in Figure 4, and we now give an explanation of the model's behavior. At almost all times, V exponentially approaches I from below with time–constant 1, and c exponentially decays towards 0 with time–constant τ. At each firing time t_n, c is incremented: $c \mapsto c + B + Cc^2$. At a time σ after firing, and assuming that the previous ISI, $t_n - t_{n-1}$, is greater than the refractory period r, V is incremented: $V \mapsto V + c$, where c is evaluated at a time σ after firing. If the previous ISI is less than the refractory period, V is not incremented. Note that the neuron will not fire if I is always less than 1.

This model was not derived from (1)-(6) in any systematic fashion, but rather was created "out of the blue" using the knowledge about the bursting mechanism from Ref. [4]. It is thus not the only minimal model the produces ghostbursting, but can be thought of as one from a family of such models [11]. Indeed, another minimal ghostbursting model with a different formulation was presented in [14].

The model (7)-(8) qualitatively reproduces many aspects of the bursting seen in (1)-(6), including the transition from periodic firing to bursting through a saddle–node bifurcation of periodic orbits. It also has far fewer parameters, and the effects of changing them on the system's behavior are more easily determined than would be the case for (1)-(6).

Because (7)-(8) is linear when the arguments of the delta functions are non–zero the dynamics can be explicitly solved during these intervals, and we can derive a piecewise two–dimensional map for $\Delta_{n+1} \equiv t_{n+1} - t_n$ and $c_{n+1} \equiv c(t_{n+1}^+)$ in terms of Δ_n and c_n:

$$\Delta_{n+1} = \begin{cases} \sigma & \text{if } \Delta_n > r \text{ and } I(1 - e^{-\sigma}) + c_n e^{-\sigma/\tau} > 1 \quad (i) \\ \sigma + \ln\left(\frac{c_n e^{-\sigma/\tau} - I e^{-\sigma}}{1 - I}\right) & \text{if } \Delta_n > r \text{ and } I(1 - e^{-\sigma}) + c_n e^{-\sigma/\tau} < 1 \quad (ii) \\ \ln\left(\frac{I}{I-1}\right) & \text{if } \Delta_n < r \quad (iii) \end{cases} \tag{9}$$

$$c_{n+1} = c_n e^{-\Delta_{n+1}/\tau} + B + C[c_n e^{-\Delta_{n+1}/\tau}]^2 \tag{10}$$

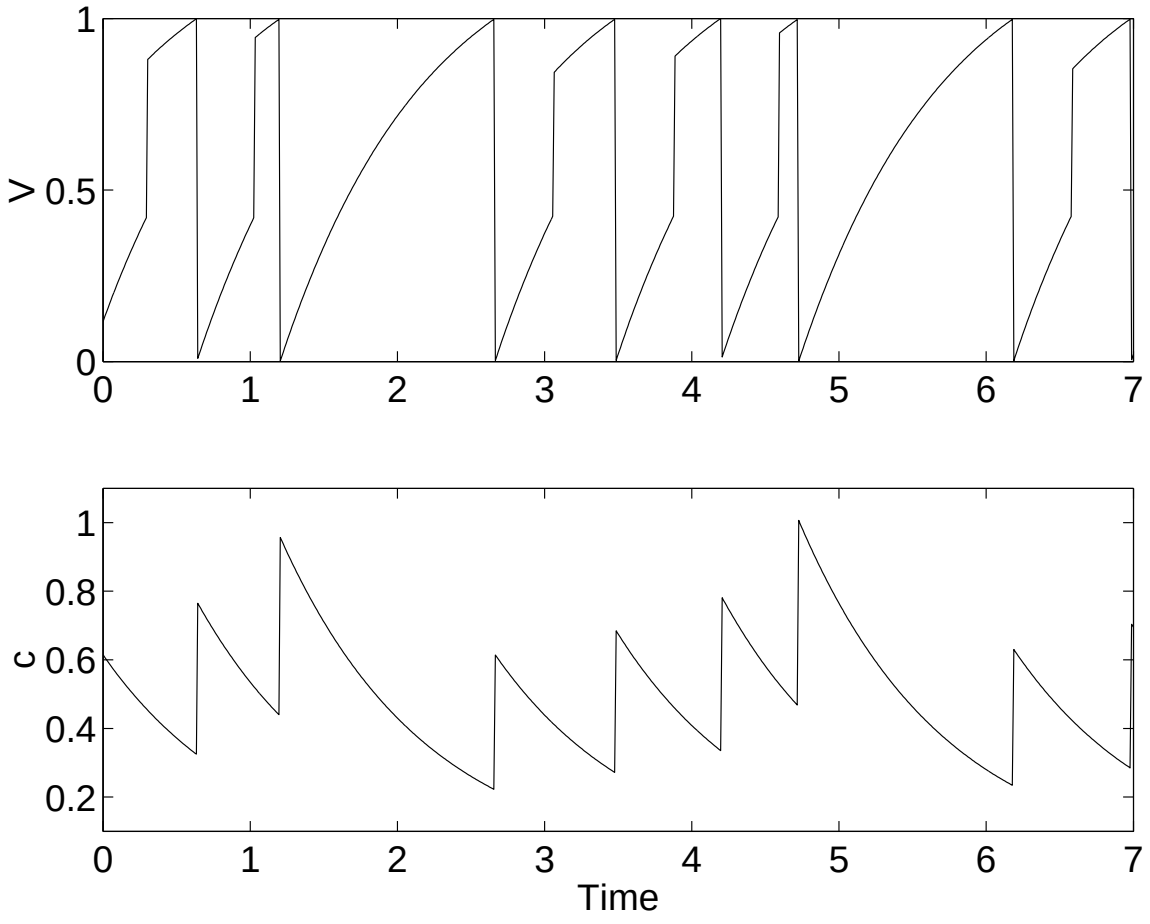

Figure 4: An example of ghostbursting in (7)-(8). Top: somatic voltage (V), bottom: auxiliary variable (c). Note the increment in V at a time σ after each firing time (except when the previous ISI was smaller than the dendritic refractory period r). The firing times occur when V reaches 1. The bursting is chaotic, as determined by the most positive Lyapunov exponent [11], thus the behavior does not repeat. Parameter values are $B = 0.35, C = 0.9, r = 0.7, \sigma = 0.4, \tau = 1, I = 1.3$.

Assuming that the injected current I is constant, the map (9)-(10) is equivalent to the system (7)-(8), but is much quicker to simulate and is also easier to analyse.

In [11] the periodic forcing of (7)-(8) (by modulating the current I) was investigated. An explicit map similar in form to (9)-(10) was derived for the case of sinusoidal modulation, although it had three variables rather than two. This map made the analytic study of resonance (Arnol'd) tongues possible, and also facilitated the study of stochastic resonance in (9)-(10).

5 Other Work

Other relevant work involving the ghostburster is now described. In Ref. [14] the minimal model (7)-(8) was modified so that the second variable controlled both the width of the dendritic action potential and the dendritic refractory period. This formulation allowed an investigation into the effects of varying both the somatic and dendritic spike widths, as would occur when potassium channels in the soma or dendrite were selectively blocked. The analytical results derived compared favourably with experiments in which this occurred, and provided further insight into the differential effects of such selective blocking.

In Ref. [10] the concept of "burst excitability", first introduced in [11], was investigated. Burst excitability is a generalization of "normal" excitability [8], in which a small perturbation causes a system to return monotonically to rest, but a large perturbation causes the system to make a stereotypical large excursion in phase space before returning to rest. Since the transition from periodic firing to bursting in (1)-(6) is via a saddle–node bifurcation, and a burst involves a large stereotypical excursion through phase space, there is an analogous form of excitability in (1)-(6). The main difference between burst excitability in (1)-(6) and normal excitability is that the large excursion is a burst, and the system returns to periodic firing after the burst, rather than to a steady state.

The effects of time–varying input to a model ghostbursting neuron were further investigated in [12]. Here, the input current to the soma was sinusoidally modulated. It was found that the modulation could switch the model neuron from bursting to periodic firing, or vice versa, depending on the frequency of forcing and the distance from the periodic/burst threshold. This could be explained by mapping resonance tongues in parameter space. Stochastic resonance was also observed in this periodically forced system, assuming that the doublet at the end of a burst was used to form the "signal".

The pyramidal cells that show burst excitability and entrainment to periodic inputs are primary sensory neurons, i.e. they receive input directly from electroreceptors on the fish's skin [2]. It is reasonable to suppose that bursts are somehow involved in signalling information about the environment of the fish to its higher brain centres, and it was discussed in [10] how burst excitability might contribute to this processing and transfer of information. For example, given the unreliability of some neural processes, a burst of action potentials could be a more robust means of signalling an event than a single action potential. Also, it may be the case that a facilitating synapse could be "tuned" to pick out the accelerating action potentials that characterize ghostbursting.

The role of the saddle–node bifurcation of periodic orbits that separates periodic from burst firing was further investigated in [6]. Here, the authors added a persistent sodium current with a slow timescale (on the order of one second) to the compartmental model in [5]. The effect of this is qualitatively the same as slowly increasing the current injected into the cell's soma, and thus results in the cell's firing frequency slowly increasing until burst discharge starts. The lengths of these bursts then slowly decrease over time. The purpose of adding this

slow current was to reproduce the behavior just described, as this is what is observed when a constant current is injected into a pyramidal cell's soma for several seconds [6]. The change in burst duration over time was understood in terms of the scaling properties associated with saddle–node bifurcations [4, 17].

In [9] the effects of varying both the coupling conductance between the soma and dendrite (g_c) and the ratio of somatic to total area (κ) in the model (1)-(6) were studied. It was found that both parameters had to be moderately large (but not too large) in order for the neuron to burst, and this was understood in terms of the previous bifurcation analysis [4].

6 Summary

We have given an outline of the stages in the analysis of "ghostbursting", a type of bursting seen in pyramidal cells from weakly electric fish. Initially, the distribution of ion channels on these cells and the underlying features of ghostbursting were determined experimentally [13, 18]. A large compartmental model was constructed and further necessary ingredients for bursting were determined [5]. This compartmental model was simplified to a two–compartment model involving six variables [4], which enabled the mathematical analysis of the bursting. Once the underlying mechanism of bursting had been determined, a "toy" minimal model was constructed [11]. This model enabled further analysis of the effects of changing parameters in the various models, and is ideal for large simulations of networks of ghostbursting neurons.

The development of the ghostburster has challenged previously held views about what is necessary for a system to show bursting [7, 16]. Now that the bursting mechanism has been characterized, future work could involve integrating the feedback circuits known to project to the pyramidal cells [1] to form a "computational loop", or studying spatially–extended arrays of such neurons with appropriate feedback [3].

Acknowledgements: I thank Anne-Marie Oswald for providing the data in Figure 1, Brent Doiron for conversations regarding this paper, and the referees for their helpful comments.

References

[1] N. J. Berman and L. Maler, Neural architecture of the electrosensory lateral line lobe: adaptations for coincidence detection, a sensory searchlight and frequency-dependent adaptive filtering, *J. Exp. Biol.* 202 (1999), 1243-1253.

[2] M. J. Chacron, A. Longtin and L. Maler, Negative interspike interval correlations increase the neuronal capacity for encoding time-dependent stimuli, *J. Neurosci.*, 21 (2001), 5328-5343.

[3] B. Doiron, M. J. Chacron, L. Maler, A. Longtin and J. Bastian, Inhibitory feedback required for network oscillatory responses to communication but not prey stimuli, *Nature* 421 (2003), 539-543.

[4] B. Doiron, C. Laing, A. Longtin and L. Maler, Ghostbursting: a novel neuronal burst mechanism, *J. Comput. Neurosci.* 12(1) (2002), 5-25.

[5] B. Doiron, A. Longtin, R. W. Turner and L. Maler, Model of gamma frequency burst discharge generated by conditional backpropagation, *J. Neurophysiol.* 86 (2001), 1523-1545.

[6] B. Doiron, L. Noonan, N. Lemon, and R. W. Turner, Persistent Na^+ current modifies burst discharge by regulating conditional backpropagation of dendritic spikes, *J. Neurophysiol.* 89 (2003), 324-337.

[7] E. M. Izhikevich, Neural excitability, spiking, and bursting, *Int. J. Bifn. Chaos* 10 (2000), 1171-1266.

[8] J. Keener and J. Sneyd. *"Mathematical Physiology"*, Interdisciplinary Applied Mathematics, Vol. 8. Springer–Verlag New York, 1998.

[9] C. R. Laing, B. Doiron, A. Longtin and L. Maler, Ghostbursting: the effects of dendrites on spike patterns, *Neurocomputing*, 44-46 (2002), 127-132.

[10] C. R. Laing, B. Doiron, A. Longtin, L. Noonan, R. W. Turner and L. Maler, Type I burst excitability, *J. Comput. Neurosci.* 14(3), (2003) 329-342.

[11] C. R. Laing and A. Longtin, A two–variable model of somatic–dendritic interactions in a bursting neuron, *Bull. Math. Biol* 64(5), (2002), 829-860.

[12] C. R. Laing and A. Longtin, Periodic forcing of a model sensory neuron, *Phys. Rev. E*, 67 (2003) 051928.

[13] N. Lemon and R. W. Turner, Conditional spike backpropagation generates burst discharge in a sensory neuron, *J. Neurophysiol.* 84 (2000) 1519-1530.

[14] L. Noonan, B. Doiron, C. R. Laing, A. Longtin and R. W. Turner, A dynamic dendritic refractory period regulates burst discharge in the electrosensory lobe of weakly electric fish, *J. Neurosci.* 23(4), (2003), 1524-1534.

[15] P. F. Pinsky and J. Rinzel, Intrinsic and network rhythmogenesis in a reduced Traub model for CA3 neurons, *J. Comput. Neurosci.* 1 (1994), 39-60.

[16] J. Rinzel and G. B. Ermentrout, Analysis of neural excitability and oscillations, in "Methods in Neuronal Modeling: From Ions to Networks" (ed. C. Koch and I. Segev), *MIT Press*, 1998.

[17] S. H. Strogatz. *"Nonlinear Dynamics and Chaos with Applications to Physics, Biology, Chemistry, and Engineering"*. Addison-Wesley, Reading, MA., 1994.

[18] R. W. Turner, L. Maler, T. Deerinck, S. R. Levinson, and M. H. Ellisman, TTX-sensitive dendritic sodium channels underlie oscillatory discharge in a vertebrate sensory neuron, *J. Neurosci.* 14 (1994), 6453-6471.